Chemical Research in Toxicology

pubs.acs.org/crt

Article

Structural and Mechanistic Investigation of the Unusual Metabolism of Nifurtimox

Dieter Lang,* Simone I. Schulz, Isabel Piel, Dieudonné T. Tshitenge, and Heino Stass

Cite This: *Chem. Res. Toxicol.* 2022, 35, 2037−2048

Read Online

ACCESS | Metrics & More | Article Recommendations | Supporting Information

ABSTRACT: The oral antiparasitic drug nifurtimox has been used to treat Chagas disease for more than 50 years. Historical studies determined that very little nifurtimox is excreted unchanged, but contemporaneous preclinical studies of radiolabeled nifurtimox found almost all of the radiolabel was rapidly excreted, suggesting that metabolism is extensive. Attempts to study nifurtimox metabolism have had limited success, yet this knowledge is fundamental to characterizing the pharmacokinetics and pharmacodynamics of the drug. We conducted *in vitro* studies using hepatic and renal sources with ^{14}C-labeled nifurtimox as substrate and obtained samples of urine, plasma, and feces from rats administered 2.5 mg/kg [^{14}C]-nifurtimox, and samples of human urine and plasma from phase 1 clinical studies in which participants received a single dose of 120 mg nifurtimox. Analysis of metabolites was done by high-performance liquid chromatography (HPLC)-high-resolution mass spectrometry (HRMS) and HRMS/MS with offline liquid scintillation counting of radiolabeled samples. Surprisingly, only traces of a few metabolites were identified from *in vitro* incubations with hepatocytes and subcellular fractions, but more than 30 metabolites were identified in rat urine, mostly with atypical mass changes. We developed an HRMS scouting method for the analysis of human samples based on the sulfur atom in nifurtimox and the natural abundance of ^{34}S, as well as a characteristic tandem mass spectrometry (MS/MS) fragmentation of nifurtimox and metabolites. Fragmentation patterns on HRMS/MS were used to propose structures for 18 metabolites (22 including stereoisomers), and based on these structures, the six most abundant products were synthesized and the structures of the synthetic forms were confirmed by HRMS and two-dimensional nuclear magnetic resonance (2D NMR). Overall, we determined that the metabolism of nifurtimox is almost certainly not mediated by typical hepatic and renal drug-metabolizing enzymes, and instead is rapidly metabolized mainly by reduction or nucleophilic attack, with some evidence of oxidation. Knowledge of the most abundant metabolites of nifurtimox affords the possibility of future studies to investigate levels of exposure and possible drug−drug interactions.

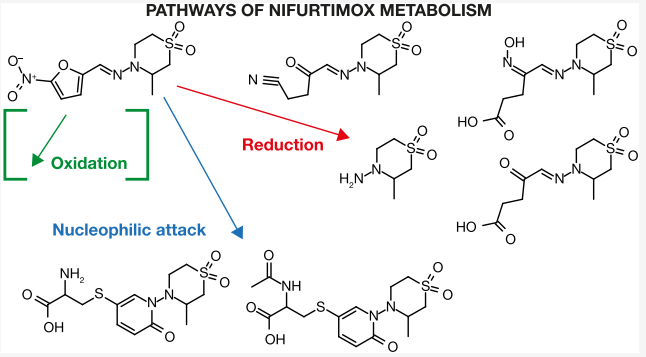

INTRODUCTION

Chagas disease is caused by the parasite *Trypanosoma cruzi*. The disease is an important cause of premature mortality in endemic regions, and it is estimated that 6−8 million individuals are infected with *T. cruzi* globally.[1,2] Nifurtimox is one of two drugs approved for the treatment of Chagas disease[2] and was first used in adults more than 50 years ago.[3,4] In 2020, it was approved by the U.S. Food and Drug Administration for the treatment of Chagas disease in all pediatric age groups,[5] based on data from the randomized phase 3 CHICO trial.[6] In 1965, when nifurtimox was first administered to adults with Chagas disease, the drug approval process was simpler and several preclinical and early clinical development studies were not performed that are now conducted routinely. In addition, the conduct of studies is always constrained by the technology available at the time. Identifying and characterizing products of drug metabolism is fundamental to the clinical development of new drug candidates, and technological improvements allow this to be done in far greater detail now than would have been possible 50 years ago. Gathering this information underpins the study of pharmacokinetic and pharmacodynamic factors such as establishing the abundance of different metabolites, characterizing their distribution and excretion profiles, and investigating whether they affect other drugs or drug-clearance mechanisms.

Despite studies that include a preliminary analysis to identify the main metabolites of nifurtimox in humans,[7] its biotransformation remains poorly understood. Historical *in vivo* studies found that the metabolism of the drug is extensive.[8,9] At 48 h after oral or intravenous (iv) dosing of

Received: June 29, 2022
Published: October 9, 2022

Table 1. HRMS Data for Nifurtimox and Metabolites M-1 to M-18

Assignment	Analzyed mass $[M+H]^+$ (m/z)	Theoretical mass $[M+H]^+$ (m/z)	Mass shift from parent (Da)	Proposed formula	Structure proposal
Parent	288.0648	288.0649	-	$C_{10}H_{14}O_5N_3S$	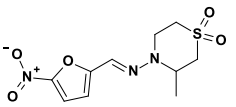
M-1	258.0905	258.0907	-30	$C_{10}H_{16}O_3N_3S$	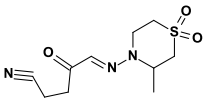
M-2	292.0959	292.0962	+4	$C_{10}H_{18}O_5N_3S$	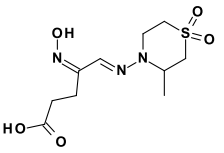
M-3	277.0852	277.0853	-11	$C_{10}H_{17}O_5N_2S$	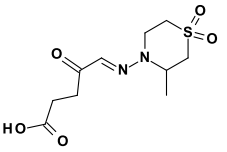
M-4	362.0837	362.0839	+74	$C_{13}H_{20}O_5N_3S_2$	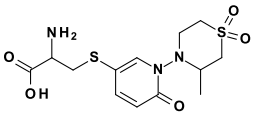
M-5	404.0942	404.0945	+116	$C_{15}H_{22}O_6N_3S_2$	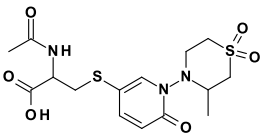
M-6	165.0692	165.0692	-123	$C_5H_{13}O_2N_2S$	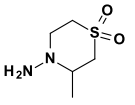
M-7	352.0993	352.0995	+64	$C_{12}H_{22}O_5N_3S_2$	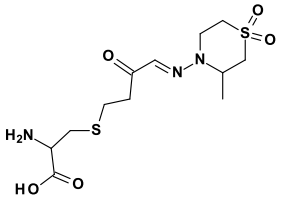
M-8	394.1100	394.1101	+106	$C_{14}H_{24}O_6N_3S_2$	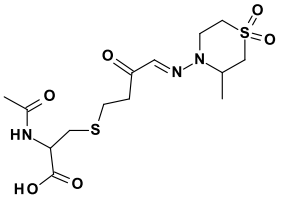
M-9	293.0800	293.0802	+5	$C_{10}H_{17}O_6N_2S$	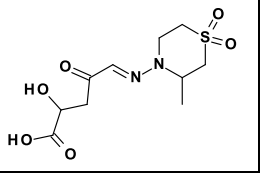

https://doi.org/10.1021/acs.chemrestox.2c00210
Chem. Res. Toxicol. 2022, 35, 2037−2048

Table 1. continued

Assignment	Analzyed mass $[M+H]^+$ (m/z)	Theoretical mass $[M+H]^+$ (m/z)	Mass shift from parent (Da)	Proposed formula	Structure proposal
M-10a/b	419.1051	419.1054	+131	$C_{15}H_{23}O_6N_4S_2$	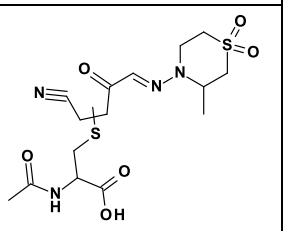
M-11	304.0595	304.0598	+16	$C_{10}H_{14}O_6N_3S$	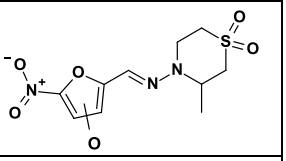
M-12	320.0543	320.0547	+32	$C_{10}H_{14}O_7N_3S$	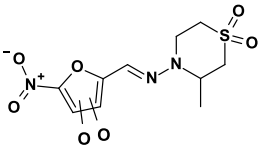
M-13a/b	336.0333[a]	336.0330[a]	+50	$C_{10}H_{14}O_6N_3S_2$	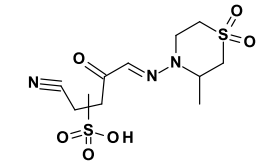
M-14	355.0278[a]	355.0275[a]	+69	$C_{10}H_{15}O_8N_2S_2$	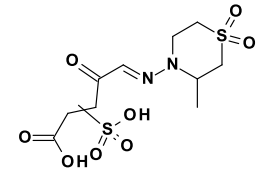
M-15	277.0847	277.0853	-11	$C_{10}H_{17}O_5N_2S$	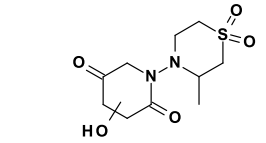
M-16	306.0750	306.0754	+18	$C_{10}H_{16}O_6N_3S$	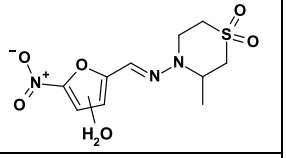
M-17a/b	256.0751	256.0750	-32	$C_{10}H_{14}O_3N_3S$	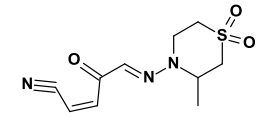
M-18a/b	548.1481	548.1480	+260	$C_{20}H_{30}O_9N_5S_2$	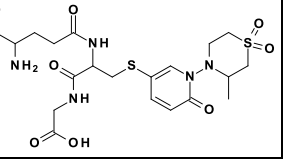

[a] $[M - H]^-$.

rats with ^{35}S-labeled nifurtimox (dose range, 2.5−25 mg/kg), more than 90% of radioactivity had been excreted (feces, 56−58%; urine, 34−38%).[8] Similarly, at 72 h after oral or iv dosing with ^{35}S-labeled nifurtimox in dogs (10 mg/kg), about 75% of

https://doi.org/10.1021/acs.chemrestox.2c00210
Chem. Res. Toxicol. 2022, 35, 2037−2048

radioactivity had been excreted. More than 10 labeled excretion products were detected on thin-layer chromatography of rat urine, as well as barely detectable levels of the parent compound, suggesting that nifurtimox was almost completely metabolized.[8] A separate but contemporaneous study of unlabeled nifurtimox in rats, dogs, and humans showed that the amount of parent compound recovered in urine was approximately 0.5% of the administered dose.[9] Based on the levels and distribution of the radiolabel, the absorption and elimination of ^{35}S-labeled nifurtimox were found to be rapid,[8] but taken together with the observation that only very low levels of unchanged nifurtimox were found in urine in the unlabeled-drug study,[9] this early evidence supported the notion that nifurtimox is rapidly and extensively metabolized. A more recent *ex vivo* study, in which rat livers were perfused in recirculation mode with a solution of nifurtimox, demonstrated that almost no parent compound remained after a 2 h incubation period and that some highly polar metabolites had accumulated. Another notable finding in this study was that samples of perfusate over time retained most of the antiparasitic activity,[10] possibly suggesting the formation of a pharmacologically active metabolite.

In a subsequent study investigating the antiparasitic activity of nifurtimox, a key step in understanding the mode of action of nifurtimox came from its biotransformation being catalyzed by nitroreductases,[11] to which its antiparasitic activity is attributable. Nitroreductases are a group of flavin cofactor-dependent enzymes that are more commonly expressed in bacterial than eukaryotic cells. They are categorized as type I (oxygen-insensitive) or type II (oxygen-sensitive) based on their ability to catalyze the reduction of nitro groups in the presence of oxygen.[12] Nifurtimox differential cytotoxicity in *T. cruzi* is attributed to activation in the parasite by a type I nitroreductase rarely found in eukaryotes but abundantly expressed in trypanosomes.[13] The action of the *T. cruzi* nitroreductase leads to the production of nitrenium ions that promote DNA strand breaks and of unsaturated open-chain nitriles that can react nonspecifically with a range of cellular components.[11,14] The parasitic type I enzyme can reduce the nitrofuran moiety of nifurtimox even in the presence of oxygen, while in contrast, the type II nitroreductase (produced by human cells and *T. cruzi*) converts nifurtimox to an intermediate that undergoes futile cycling in the presence of oxygen. Futile cycling regenerates the parent compound and releases superoxide anions.[11,12] Indeed, *in vitro* investigation of the behavior of nitro-aryl drugs in a rat liver microsomal system demonstrated the production of reactive oxygen species on the addition of nifurtimox.[15] Apart from pharmacological activation by bacterial nitroreductases, the metabolism of nifurtimox and the pathways and enzymes involved remain mostly unknown in preclinical model species and humans.

The objective of this study was to characterize the metabolism of nifurtimox in rats and humans. Therefore, we used radiolabeled nifurtimox for rat and human *in vitro* studies and *in vivo* studies in rats. In addition, we developed a new metabolite scouting strategy using high-resolution mass spectrometry (HRMS) and analyzed urine and plasma from patients who received nifurtimox to identify, elucidate, and propose the structures of many of these products and to understand the mechanisms underpinning their formation.

EXPERIMENTAL PROCEDURES

Materials. Radiolabeled substrate [^{14}C]-nifurtimox [(*E*)-*N*-(3-methyl-1,1-dioxo-1,4-thiazinan-4-yl)-1-(5-nitrofuran-2-yl)-methanimine] was synthesized with a specific activity of 6.40 MBq/mg by American Radiolabeled Chemicals, Inc. (St. Louis, MO) incorporating ^{14}C in the imine moiety. Unlabeled metabolites subsequently designated M-1 to M-5 (Table 1) were synthesized by Bayer AG (Wuppertal, Germany) as reference compounds for structure confirmation (see Supporting Methods); metabolite M-6 (Table 1), which is a synthetic precursor of nifurtimox, was already available (Bayer AG; Wuppertal, Germany).

High-performance liquid chromatography (HPLC)-grade acetonitrile, ammonium formate, and formic acid were from Merck Group (Darmstadt, Germany). Liquid scintillant cocktails Ultima Gold and Ultima-Flo were from PerkinElmer (Überlingen, Germany). Acetyl coenzyme A (AcCoA), recombinant *Escherichia coli* nitroreductase (expressed in *E. coli*; specific activity ≥100 U/mg protein), and Williams' E cell-culture medium were from Sigma-Aldrich (Steinheim, Germany). All other chemicals and reagents were sourced commercially at analytical grade or its equivalent. Human kidney S9 fraction was from Bioreclamation (Hicksville, NY). Rat liver and kidney S9 fractions and rat liver cytosol were prepared at Bayer AG (Wuppertal, Germany) using methods reported elsewhere.[16] Subcellular fractions were stored at −80 °C. Cryopreserved primary human and Wistar rat hepatocytes were from Lonza (Basel, Switzerland) and were stored under liquid nitrogen. Fresh, heparinized human blood and human feces were from healthy volunteers. Human urine was collected from patients with Chagas disease immediately before or after receiving a single dose of nifurtimox 120 mg in a phase 1 clinical study (NCT02606864).[14] Pooled human plasma was from blood samples collected per protocol from six adult patients with Chagas disease during the 24 h after receiving a single 120 mg dose of nifurtimox in another phase 1 clinical study (NCT03350295).[17] Plasma, urine, and fecal samples were from absorption, distribution, metabolism, and excretion (ADME) studies conducted at Bayer AG, in which male Wistar rats received an oral dose of 2.5 mg/kg [^{14}C]-nifurtimox (publication in preparation). All experiments were performed in accordance with the respective local legal animal protection and other effective government requirements.

Liquid scintillation spectrometers Tri-Carb 2910 TR and 4910 TR were from PerkinElmer, Waltham, MA. HPLC-MS-Orbitrap (LC system 1260 or 1290 with diode array detector) was from Agilent (Waldbronn, Germany). Q-Exactive Plus and Orbitrap Fusion Lumos Tribrid HRMS instruments with heated electrospray ionization (ESI) source were from Thermo Fisher Scientific (Bremen, Germany).

Incubation Conditions for the Investigation of [^{14}C]-Nifurtimox Metabolism in Recombinant and *In Vitro* Test Systems. Stock solutions of [^{14}C]-nifurtimox in acetonitrile were diluted to 1−20 μM in each reaction (final acetonitrile concentration 1% [v/v]) and incubated with 4 U of recombinant *E. coli* type I nitroreductase in 50 mM potassium phosphate buffer pH 7.4 containing 1 mM ethylenediaminetetraacetic acid (EDTA) and 1 mM nicotinamide adenine dinucleotide plus hydrogen (NADH) as a cofactor for up to 90 min at 37 °C. Subcellular fractions (rat liver S9 and cytosol; human kidney S9) were incubated under similar conditions using a nicotinamide adenine dinucleotide phosphate plus hydrogen (NADPH)-generating system (1 mM NADP, 5 mM glucose-6-phosphate, 1.5 U/mL glucose-6-phosphate dehydrogenase). Enzymatic acetylation by rat or human S9 fractions was investigated by the addition of 1 mM acetyl-CoA (AcCoA). Suspension cultures of primary rat or human hepatocytes in Williams' E medium were incubated with 1 or 10 μM [^{14}C]-nifurtimox at 37 °C for up to 4 h. To investigate anaerobic metabolism in hepatocytes, culture flasks and Williams' E medium were flushed with nitrogen before the addition of [^{14}C]-nifurtimox. For stability in human blood or urine, 5 and 20 μM [^{14}C]-nifurtimox was incubated at 37 °C for 1.5 h (in blood) or up to 48 h (in urine).

For anaerobic stability studies in human feces, 8.8 μM [^{14}C]-nifurtimox was incubated with a suspension of approximately 20% (w/v) fresh feces dispersed in degassed phosphate buffer pH 7.0, and

https://doi.org/10.1021/acs.chemrestox.2c00210
Chem. Res. Toxicol. 2022, 35, 2037−2048

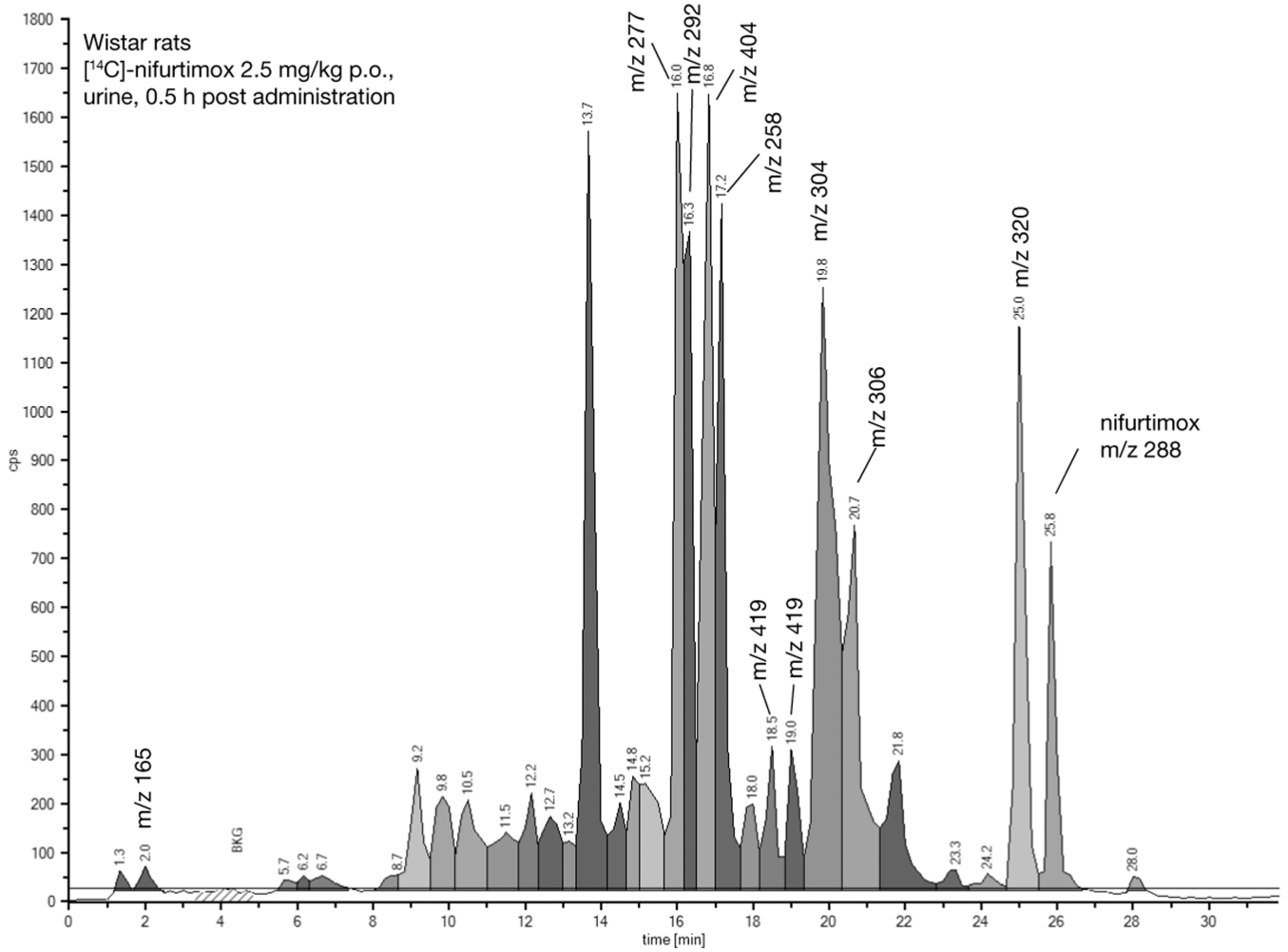

Figure 1. Profile of radiolabeled products and the m/z values of the protonated $[M + H]^+$ species in rat urine at 0.5 h post oral administration of 2.5 mg/kg [^{14}C]-nifurtimox.

with degassed phosphate buffer pH 7.0 as a control, under nitrogen at 37 °C for 20 h. The susceptibility of nifurtimox to chemical reduction was investigated by mixing [^{14}C]-nifurtimox at a final concentration of 20 μM with $SnCl_2$ and separately with sodium dithionite. Susceptibility to conjugation with thiol-containing nucleophiles was investigated by incubation of 20 μM [^{14}C]-nifurtimox with 1 mM cysteine and with 1 mM *N*-acetylcysteine for 1 h at 37 °C.

Sample Preparation for Analysis. Nifurtimox was stable under most conditions relevant for sample handling, except handling under light protection. For all incubations, reactions were stopped at the end of the incubation period by the addition of acetonitrile to 30−75% (v/v) and either analyzed directly or stored at −20 °C until analysis. Before analysis, precipitated protein was pelleted by centrifugation at approximately 13 000*g* for 5 min at room temperature. Supernatants were removed and aliquots were taken for analysis by HPLC coupled to HRMS and with offline [^{14}C]-radio-detection.

Analytical Method for the Separation and Detection of [^{14}C]-Labeled Metabolites. Samples were analyzed by HPLC using a 150 × 2.0 mm Prodigy ODS-3 column (particle size, 3 μm; pore size, 100 Å), and a gradient elution applied for metabolite separation (solvent A, 0.05% [v/v] aqueous formic acid; solvent B, 0.05% [v/v] formic acid in acetonitrile; 0 min, 0% B; 4 min, 0% B; 26 min, 27% B; 27 min, 90% B; 29 min, 90% B; 31 min, 0% B; post time, 3 min) at a flow rate of 0.3 mL/min at 40 °C. Radio-detection was off-line with the collection of timed HPLC fractions (10 s) and addition of scintillation cocktail (Ultima Flo AP). Liquid scintillation counting (LSC) was performed using a PerkinElmer 1450 Microbeta Plus or 2450 Microbeta 2 microplate counter (5 min). Radioactivity of liquid samples was measured in a Tri-Carb 2910 TR or 4910 TR, with automatic quench correction by the external standard channel ratio method, at 13 °C. Scintillation data were evaluated using Wallac-TopCount Connector, v2.0.5.0 (Bayer Business Services GmbH, Leverkusen, Germany). Background signal was determined as the mean of 10 sample fractions.

Mass Spectrometry. HRMS after HPLC (HPLC-HRMS) used positive/negative ESI mode (ion source voltage: positive, 3500 V; negative, −2000 V) in the mass range 50−1500 Da in full-scan mode with a resolution of 240 000. Source temperature was typically 50−250 °C, capillary temperature was 300 °C, and collision energy was in the range 20−45 eV.

Structure Confirmation by ^{1}H and ^{13}C Nuclear Magnetic Resonance (NMR) Spectroscopy. Nuclear magnetic resonance (NMR) spectra were acquired using 500 and 600 MHz spectrometers (Bruker Corporation, Billerica, MA) equipped, respectively, with 1.7 mm Cryo-TCI and 5 mm Cryo-DCH probes (Bruker Corporation). Synthetic metabolites M-1 to M-5 (Table 1) were dissolved in dimethyl sulfoxide-d_6 at a final concentration of 10−100 mM. ^{1}H NMR spectra were collected at 500 MHz (M-1, M-4, M-5) or 600 MHz (M-2, M-3), and ^{13}C NMR spectra were collected at 126 MHz (M-1, M-4, M-5) or 151 MHz (M-2, M-3); 2D spectra (^{1}H, ^{13}C-heteronuclear single quantum coherence [HSQC]; ^{1}H, ^{13}C-heteronuclear multiple bond correlation [HMBC]; ^{1}H, ^{1}H-COrrelated SpectroscopY [COSY]) were also acquired for structure elucidation. TopSpin 3.6 (Bruker Corporation) was used for data acquisition, processing, and analysis.

https://doi.org/10.1021/acs.chemrestox.2c00210
Chem. Res. Toxicol. 2022, 35, 2037−2048

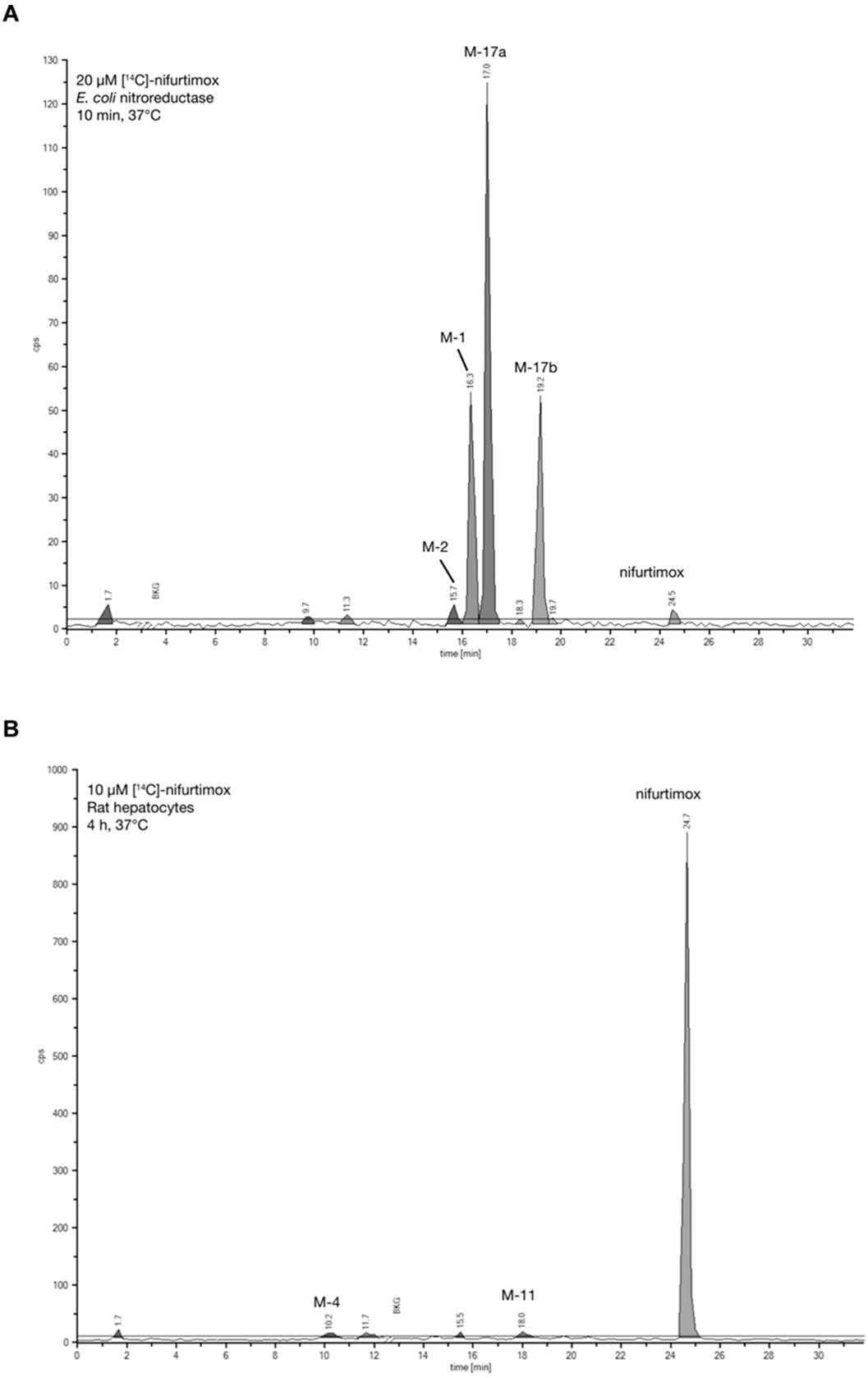

Figure 2. continued

https://doi.org/10.1021/acs.chemrestox.2c00210
Chem. Res. Toxicol. 2022, 35, 2037−2048

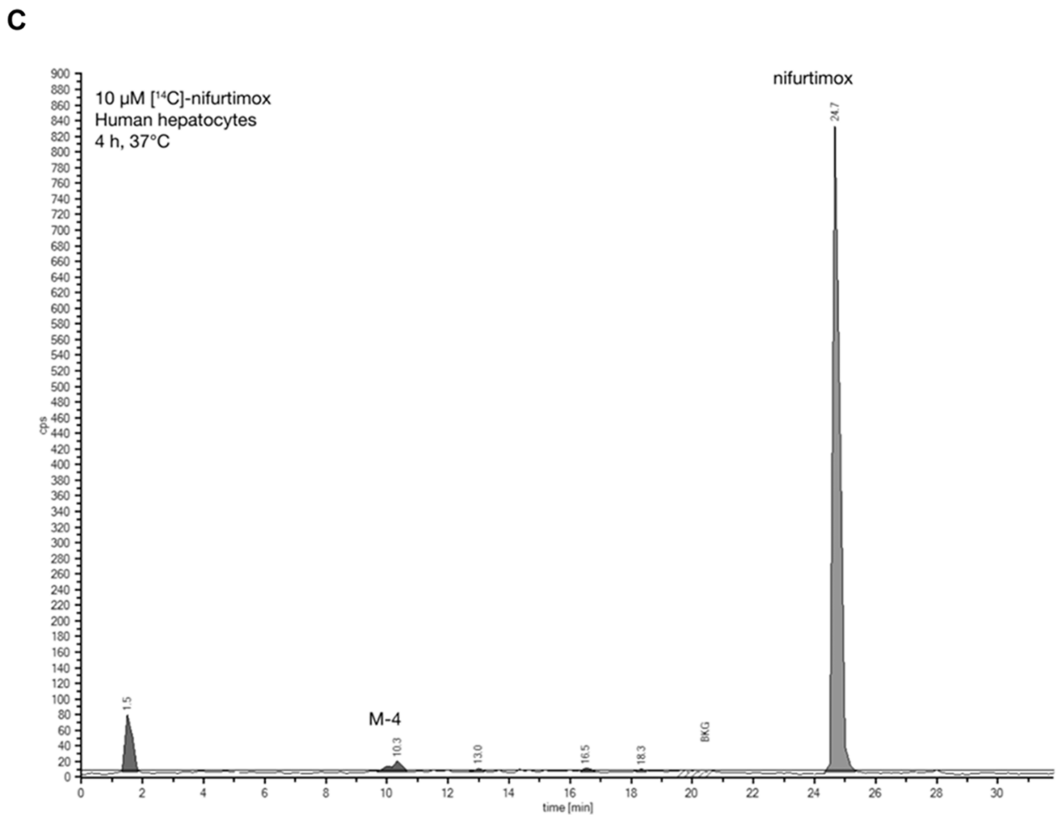

Figure 2. Metabolite profiles after incubation of [^{14}C]-nifurtimox with nitroreductase (A), and rat and human hepatocytes (B, C) *in vitro*.

RESULTS

Analysis of Urine from Rats after Administration of [^{14}C]-Nifurtimox. Separation of radiolabeled components by HPLC/HRMS with off-line LSC detection showed that the metabolism of nifurtimox *in vivo* is highly complex. More than 30 nifurtimox-related metabolites were detected (Figure 1) in urine collected 0.5 h after oral administration of [^{14}C]-nifurtimox in a rat ADME study (manuscript in preparation), indicating extensive and rapid metabolism.

Based on the unusual mass changes relative to nifurtimox (m/z 288), almost all of the products seemed to be uncommon metabolites, complicating both structure elucidation and deduction of the likely metabolic reactions and pathways involved. We therefore screened different test systems *in vitro* to determine how the various metabolites might form.

Recombinant and *In Vitro* Test Systems. Metabolites identified after incubation of [^{14}C]-nifurtimox with different test systems incorporating different cofactors (NADH, NADPH) are summarized in Table S1. A few metabolites of nifurtimox were identified in these experiments, and they were only formed in very low or trace amounts. The exception was incubation with recombinant *E. coli* oxygen-insensitive nitroreductase, in which [^{14}C]-nifurtimox was rapidly converted to four detectable products (Figure 2A) that were subsequently designated (Table 1) M-1, M-17a, and M-17b (stereoisomers), and M-2 (very low levels). This confirms the previously reported metabolic activation to metabolites including unsaturated (M-17a/b) and saturated (M-1) open-chain nitriles.[11] Among the subcellular fractions tested as *in vitro* models of drug metabolism, [^{14}C]-nifurtimox was unaltered after incubation for 1 h with rat liver cytosol or with human kidney S9 fraction. Low levels of M-11 were detected after incubation with rat liver S9 fraction (Figure S1). The drug-metabolizing activity of rat and human hepatocyte suspensions as test models of liver metabolism was first confirmed by incubation with prototypic substrates. However, when incubated with 1 μM [^{14}C]-nifurtimox, only the parent compound was detected after 4 h with rat or human cells (data not shown). Incubation of rat hepatocytes with 10 μM [^{14}C]-nifurtimox for 4 h yielded low levels of M-4 and M-11 (Figure 2B). Low levels of M-4 were also detected in the incubation of 10 μM [^{14}C]-nifurtimox with human hepatocytes after 4 h (Figure 2C). At the same concentration of [^{14}C]-nifurtimox under reducing conditions (incubation with human cells under nitrogen), only the parent compound was detected after 2 h (data not shown). Overall, these *in vitro* investigations neither reflected nor supported the rapid and extensive metabolism of nifurtimox that was observed in rats, so we developed a novel metabolite scouting strategy that could be applied to urine and plasma from patients.

Metabolite Scouting in Human and Rat Urine and Plasma. Analysis of the ^{14}C-labeled metabolites in rat urine yielded specific measured masses for nifurtimox-related products that could be used to pinpoint candidate unlabeled metabolites in urine from patients. However, the comparison and correlation of metabolite signals in the rat *versus* human samples seemed poor, suggesting that there may be additional metabolites in human urine. Therefore, a novel HRMS-based method was applied to the human samples that took advantage of the single sulfur atom in nifurtimox and the natural abundance of the ^{34}S isotope to identify metabolites.

Nifurtimox and its metabolites showed characteristic fragmentation at the hydrazone moiety to form two characteristic products containing the dioxidothiomorpholine moiety

https://doi.org/10.1021/acs.chemrestox.2c00210
Chem. Res. Toxicol. 2022, 35, 2037−2048

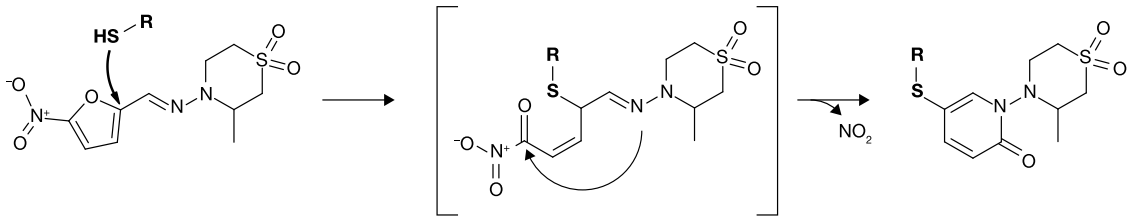

Figure 3. Proposed mechanism for nucleophilic attack of nifurtimox by thiol-containing compounds.

with m/z 148.0427 ($C_5H_{10}NO_2S$) or 150.0583 ($C_5H_{12}NO_2S$). For scouting and identification of metabolites, urine and plasma samples from humans and rats were analyzed by HRMS in full-scan mode with all-ion fragmentation (AIF) in positive ionization mode. The two characteristic fragments were then extracted from the AIF scans in high-resolution mode with a width of 5−10 parts per million (ppm). At retention times where one or both fragment signals were seen, the full-scan trace was browsed for a potential precursor at the corresponding retention time. The presence of at least one sulfur atom was the major criterion used to identify the correct precursor. The presence of a sulfur atom was confirmed by the identification of an accompanying ion species with a characteristic mass difference of 1.995 Da, attributable to the natural abundance of ^{34}S (approximately 5%) relative to the most abundant isotope, ^{32}S. All potential precursors detected in this manner were further characterized by extended separate HRMS/MS experiments to check whether they were nifurtimox-related.

In total, 14 metabolites (15 including stereoisomers) that were related to the parent compound were identified using HPLC-HRMS and HRMS/MS in urine from patients who had received nifurtimox in a clinical study:[14] M-1 to M-9 (inclusive), M-10a/b, M-11, M-12, M-15, and M-16. Of these, M-1 to M-6, inclusive, were identified as the most abundant nifurtimox metabolites based on the HRMS signal; only trace quantities of the parent drug were detected. Qualitative analysis of plasma samples from a group of patients who had received nifurtimox in a different clinical study[17] identified the same 15 metabolites, and of these, M-1 to M-6 inclusive were again the most abundant products. Products M-13a/b and M-14 were identified in rat-derived samples, as noted earlier, M-17a/b were products of metabolism by type I nitroreductase, and M-18a/b were mainly found in incubations with human blood.

Four metabolites out of M-1 to M-18 were interpreted as stereoisomers because each appeared twice, with identical masses and molecular formulae but with chromatographically separate peaks. Thus, in total, 22 metabolites, including isomers, were identified as clearly nifurtimox-related. The signals detected could be grouped as 10 metabolites (11 including stereoisomers) that contained one sulfur atom (M-1, M-2, M-3, M-6, M-9, M-11, M-12, M-15, M-16, M-17a/b) and eight metabolites (11 including stereoisomers) that contained two sulfur atoms (M-4, M-5, M-7, M-8, M-10a/b, M-13a/b, M-14, M-18a/b). The second sulfur atom was suspected to originate from conjugation with thiol-containing compounds.

Metabolite Structure Elucidation by HRMS and HRMS/MS. Together with information from NMR (see below) and reference metabolites, metabolite structures were proposed based on the molecular formula generated in the HRMS analysis, their mass change relative to the mass of the parent drug, and their fragmentation patterns in tandem mass spectrometry (MS/MS) spectra. Metabolites were each assigned an "M" number, lower numbers representing those most abundant, with suffixes "a" and "b" for stereoisomers. The measured protonated molecular exact masses, theoretical exact masses, mass shift to parent drug, and empirical formulas of the 22 metabolites (including stereoisomers) identified in the various analyses, and their proposed structures based on HRMS/MS fragmentation data, are shown in Table 1. The measured and theoretical exact masses corresponded to each other with a high degree of accuracy. Structure elucidation and the fragmentation patterns of the metabolites are summarized in Figure S2 and accompanying text. Synthetic forms of the most abundant metabolites (M-1 to M-6) yielded spectra from HRMS/MS analyses that corroborated the data from scouting (Figure S2).

The nitro moiety of nifurtimox is only preserved in three small metabolites (M-11, M-12, and M-16). It has been lost from all other metabolites, by reduction, subsequent ring opening and rearrangement (as described for the formation of M-1[11]), or (as proposed in Figure 3) nucleophilic attack by thiol-containing compounds, for example, by cysteine at the furan 2-position, with subsequent ring opening, rearrangement, then ring closure with NO_2 as a leaving group.

Structure Elucidation by NMR, Infrared, and Raman Spectroscopy. Structures for a subset of the synthetic metabolite standards (M-1 to M-5) were unambiguously determined by analysis of 1D and 2D NMR spectra (Figure S3A,B and accompanying text). A shift characteristic of a quaternary carbon in the nitrile group of M-1 was seen on ^{13}C NMR and was corroborated by infrared and Raman spectroscopies (Figure S4A,B). Also, ring closure in the proposed mechanism for the formation of M-4 and M-5 following thiol-based nucleophilic attack was corroborated by the HMBC cross peak that was observed between H10 and C18 in M-4 and between H10 and C20 in M-5 (Figure S3A). The structures of nifurtimox and M-6 (used in the synthesis of nifurtimox) are known.

Stability *Ex Vivo* in Human Urine and Feces. Analyses of human and rat *in vivo* samples separately yielded evidence that nifurtimox is unstable in excreta and that this instability may contribute to the complexity of the metabolite profile. Therefore, the stability of nifurtimox was investigated when added to human urine, and to suspensions of fresh human feces under anaerobic conditions. [^{14}C]-Nifurtimox was added at a final concentration of 5 μM to samples of human urine collected before dosing from patients in a phase 1 clinical trial of nifurtimox,[14] and the metabolite profile was characterized over time while incubated at 37 °C. At 48 h most of the parent compound was depleted and metabolite M-1 was the dominant product (Figure S5A,B). [^{14}C]-Nifurtimox (8.8 μM) was converted into labeled metabolite M-1 and unlabeled metabolite M-6 when incubated with human feces. The parent

https://doi.org/10.1021/acs.chemrestox.2c00210
Chem. Res. Toxicol. 2022, 35, 2037−2048

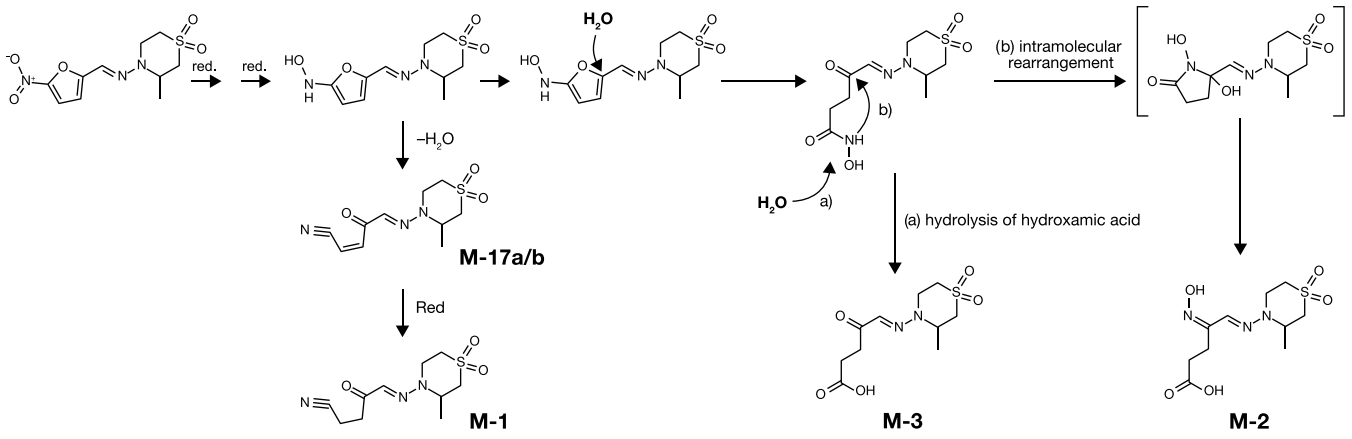

Figure 4. Proposed mechanism for the formation of M-1,[11] and M-2 and M-3 by direct ring opening or nucleophilic attack of water and hydrolysis/rearrangement of the hydroxylamine intermediate formed by a two-step reduction of nifurtimox.

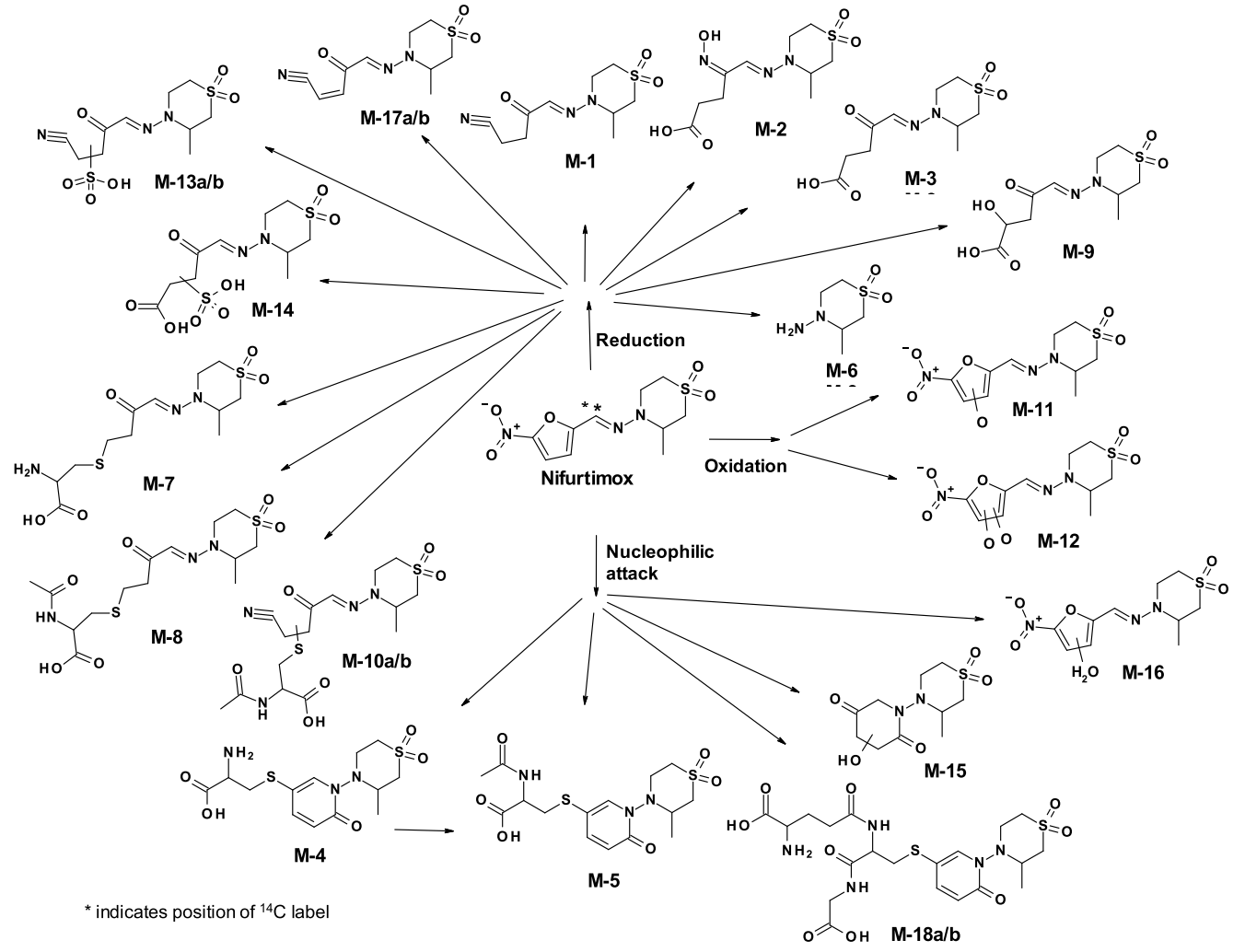

Figure 5. Main metabolic pathways of nifurtimox.

compound was unchanged when incubated under the same conditions in a buffer control (Figure S5C,D).

Further Investigations *In Vitro* to Elucidate Mechanisms of Metabolite Formation. Given the rapid metabolism of nifurtimox by nitroreductase to form M-1 and traces of M-2 (Figure 2A), the susceptibility of [^{14}C]-nifurtimox to inorganic reducing agents was investigated *in vitro*. Incubation of nifurtimox with $SnCl_2$ yielded mainly M-1, with small amounts of M-2 and M-3; unlabeled M-6 was also separately detected by HRMS (Figure S6A). Incubation with sodium dithionite gave similar results (data not shown). The mechanism for the formation of the unsaturated open-chain

https://doi.org/10.1021/acs.chemrestox.2c00210
Chem. Res. Toxicol. 2022, 35, 2037−2048

nitrile M-1 is proposed to be *via* a hydroxylamine intermediate and the unsaturated form M-17a/b.[11] Besides the ring opening of this hydroxylamine intermediate, we propose a nucleophilic attack of water at the furan ring leading, *via* ring opening, to an aliphatic hydroxamic acid, which either hydrolyzes to M-3 or rearranges to form the oxime derivative M-2 (Figure 4).

Structure elucidation by HRMS/MS and NMR indicated that M-4 and M-5 are derivatives of nifurtimox conjugated with cysteine and N-acetylcysteine, respectively, and therefore [^{14}C]-nifurtimox was incubated at 37 °C in the presence of 1 mM cysteine and *N*-acetylcysteine without any enzymes. After 1 h incubation, around 50% of nifurtimox was converted to M-4 and M-5 (Figure S6B). This confirmed that nifurtimox is susceptible to reaction with thiol-containing nucleophiles (see proposed mechanism in Figure 3). M-4 was identified after incubation of nifurtimox with hepatocyte suspensions, deriving from reaction with cysteine in Williams' E medium. Incubation of 20 μM [^{14}C]-nifurtimox for 1.5 h in whole human blood with no supplementation of cysteine or cofactors also yielded low levels of M-4; additionally, this incubation yielded traces of two glutathione conjugates M-18a and M-18b (Figure S6C). Analogous to the mechanism for the formation of M-4, the HRMS fragmentation pattern for M-18a/b indicated that these products are formed following nucleophilic attack by glutathione, with rearrangement accounting for the stereoisomers. M-18a/b were also detected in trace amounts in plasma from patients receiving nifurtimox.

The ubiquity of cysteine explains why M-4 could form *in vivo*, but *N*-acetylcysteine is not typically present *in vivo* in significant quantities. In addition, M-4 was more prevalent than M-5 in plasma, and M-5 was more prevalent than M-4 in urine. To test whether M-4 could be converted to M-5 in the kidney, M-4 was incubated with human and rat kidney S9 fractions supplemented with AcCoA as a co-factor for acetylation. In both test systems, M-4 was efficiently converted to M-5 in the presence, but not the absence, of AcCoA (Figure S6D,E).

Overall, as visualized in Figure 5, three main metabolic pathways of nifurtimox were identified: First, reduction of the nitro moiety and rearrangement leading to a variety of metabolites, 14 of which (including stereoisomers) have been identified and structures proposed; second, nucleophilic attack, most likely at the furan 2-position, leading to rearranged conjugation products, in most cases with thiol-containing reaction partners (six metabolites including stereoisomers); and third, small amounts of products of oxidation at the furan moiety (two metabolites).

DISCUSSION

Here, we report the first detailed analysis of the metabolism of nifurtimox in humans and rats. In total, we detected at least 30 nifurtimox-related products, proposed structures for 18 (22 including stereoisomeric forms), and confirmed the structures of the six most abundant products (M-1 to M-6). Among the metabolites we characterized, 11 (14 including stereoisomers M-1, M-2, M-3, M-6, M-7, M-8, M-9, M-10a/b, M-13a/b, M-14, M-17a/b) were generated from the parent compound by reductive ring opening, five (six including stereoisomers M-4, M-5, M-15, M-16, M-18a/b) by reactions with nucleophiles, and two by oxidation (M-11, M-12; Figure 5).

Structural information for nifurtimox metabolites was primarily gained from *in vivo* samples from rats and humans, and notably, biotransformation in both was similar, showing a highly complex pattern with many derivatives. Accordingly, we first tried to study this metabolism using state-of-the-art *in vitro* methods, but the approach proved frustrating. Despite applying different subcellular fractions and cofactors, hepatocytes, and both aerobic and anaerobic conditions, no significant metabolite formation redolent of that seen *in vivo* was identified *in vitro*. These strikingly different metabolite profiles essentially preclude the use of *in vitro* models as surrogates of nifurtimox biotransformation pathways. Based on this evidence, we have determined that nifurtimox metabolism is not mediated by typical drug-metabolizing enzymes such as the cytochrome P450 isoforms or UDP-glucuronosyltransferases, and thus biotransformation occurs to a great extent independently of typical hepatic and renal drug-metabolizing enzymes. Consistent with our findings, one *in vitro* study has reported that biotransformation of nifurtimox did not occur in liver microsomes.[18]

Our characterization of synthetic forms of the proposed structures of M-1 to M-6 by HRMS yielded spectra identical to those obtained during scouting, and we corroborated the structures of the synthetic forms of M-1 to M-5 separately by NMR analysis. Nifurtimox metabolites in human urine have been characterized by another group using low-resolution MS/MS.[7] Some of their proposed structures were different from those we report here, but confirmation of the proposed structures with a second analytical method or by characterization of synthetic forms seems not to have been undertaken.

We did show *in vitro* that nifurtimox is a substrate for nitroreductase, yielding M-1, small amounts of M-2, and stereoisomers M-17a and M-17b. This confirms the conversion of nifurtimox by nitroreductase that has been previously reported,[11] forming pharmacologically active metabolites including unsaturated (M-17a/b) and saturated (M-1) open-chain nitriles. The study showed that the antiparasitic activity of nifurtimox is most likely attributable to the formation of the unsaturated open-chain nitrile within the trypanosome that is a precursor of M-1.[11] Production of M-1, which is one of the more abundant reductive metabolites, has been reported previously in another study of nifurtimox metabolism.[7] The process of reduction, ring opening, and rearrangement with the loss of a nitro group, as described for M-1, was a common biotransformation mechanism for 14 of the metabolites characterized. We also propose a mechanism for the formation of M-2 and M-3 in parallel with M-1 by an alternative hydrolysis/rearrangement pathway of the hydroxylamine intermediate, as shown in Figure 4. The formation of this hydroxylamine intermediate by a two-step reduction of the nitro moiety has been described previously.[11] It remains unknown whether this occurs with or without enzymatic involvement, but the conversion of nifurtimox to M-1, M-2, M-3, and M-6 upon incubation with $SnCl_2$ *in vitro* demonstrates the lability of nifurtimox under reducing conditions.

In addition to the group of metabolites generated by reduction of the hydrazone or nitrofuran moiety of nifurtimox, another group appears to have been generated by direct interaction with thiol-containing nucleophiles, including cysteine (producing M-4) and glutathione (producing stereoisomers M-18a/b). The mechanism we propose (nucleophilic attack at the furan 2-position, ring opening, rearrangement, then ring closure with the loss of a nitro group; Figure 3) is supported by all HRMS data, by structural NMR data, and by

https://doi.org/10.1021/acs.chemrestox.2c00210
Chem. Res. Toxicol. 2022, 35, 2037−2048

the fact that M-4 formed without prior metabolic activation. Levels of cysteine in mammalian systems render its interaction with nifurtimox very likely. Cysteine is ubiquitous in mammalian systems and glutathione is synthesized from intracellular cysteine. Both M-4 and M-18a/b were detected after the addition of nifurtimox to human blood, and M-4 was detected on incubation of nifurtimox with primary hepatocyte suspensions. However, M-4 was also generated *in vitro* by incubation of nifurtimox with cysteine in the absence of enzyme, so it seems probable that M-4 and M-18a/b are formed nonenzymatically *in vivo*. Detection of cysteine and *N*-acetylcysteine-containing metabolites, albeit with proposed structures different from ours, has been previously reported in urine from patients treated with nifurtimox.[7] Incubation of nifurtimox *in vitro* with *N*-acetylcysteine produced M-5, but *N*-acetylcysteine is not found in significant quantities *in vivo*.

Analyses of human samples showed that M-4 was more prevalent in plasma than in urine and M-5 was more prevalent in urine than in plasma, so we speculated that N-acetylation of M-4 occurred in the kidneys before excretion. Incubation of M-4 and the acetylation co-factor AcCoA with renal S9 fractions from humans and rats yielded M-5, implying that N-acetylation of the cysteine-derivatized metabolites depends on the activity of endogenous renal transacetylases such as human *N*-acetyltransferase 8, which acetylates cysteine-S conjugates as part of the mercapturate detoxification pathway.[19] As one of the more abundant metabolites, M-5 could also be considered as one final detoxification step in nifurtimox metabolism.

Interaction with thiol-containing nucleophiles after reductive ring opening of nifurtimox may also account for M-7 and its N-acetylated derivative M-8 (cysteine thioether derivatives). Similarly, stereoisomers M-10a and b could both be N-acetylcysteine derivatives of the unsaturated nitrile M-17a/b. The *N*-acetylcysteine derivatives M-5 and M-10a/b were detected in rat urine; M-5 and trace amounts of the other *N*-acetylcysteine derivative, M-8, were detected in human urine.

We determined that nifurtimox is unstable in human excreta. The formation of M-1 and M-6 when nifurtimox was added to a suspension of fresh human feces indicated reductive, most likely microbial, metabolism possibly attributable to bacterial reductases. Unpublished data indicate that the instability of nifurtimox seen in human urine and feces is also observed in rats. Sulfonyl derivatives M-13a/b and M-14 were both detected in feces collected from rats after nifurtimox administration, but samples of human feces from patient studies were not available to confirm whether the same metabolites are formed. M-13a/b and M-14 seem to be sulfonyl derivatives of the unsaturated nitrile stereoisomers M-17a/b and M-3, respectively.

This study has limitations. Although detection and structure elucidation of ^{14}C-labeled products were very informative, searching for structures in nonradiolabeled samples is challenging, so some metabolites may have been missed. The action of nitroreductases represents the initial step in the activation of nifurtimox to exert its pharmacological effect. In the biotransformation studies, the intermediate formed after initial nitro reduction was not accessible and the known unsaturated nitrile (M-17a/b) could not be observed *in vivo*. Therefore, all of the nifurtimox metabolites identified represent downstream products, most probably deriving not from a bacterial nitroreductase but from other as yet unidentified reductases, or from nonenzymatic reductive processes. Moreover, it is difficult to distinguish between metabolites and degradation products owing to the observed instability of nifurtimox, and further studies would be needed to address this. It is worth noting that almost no nifurtimox is excreted in an unchanged form in rat urine or feces, nor in human urine, and given the findings of our stability studies, none would be expected in feces from patients receiving nifurtimox. The low levels of excretion in urine agree with previous reports of at most 0.5% of the administered dose being detectable.[9]

It has been speculated for many years that nifurtimox-related adverse effects and toxicities have their origin in the reduction of the nitrofuran moiety which, through the production of reactive species such as free radicals, superoxide anions, nitroradicals, or even nitrenium ions, leads to oxidative stress. Our study supports the view that the reduction of the nitrofuran moiety, which leads to at least 14 identifiable metabolites, is one of the major biotransformation pathways for nifurtimox. However, because the study analyzed clinical samples, it is not possible to distinguish whether the initial reduction of the nitrofuran took place in the trypanosomes or elsewhere in infected patients. In addition, we found that the nitrofuran moiety appears to bear some electrophilic reactivity and is easily attacked by small thiol-containing molecules such as cysteine. This leads *via* the M-4 pathway to rearranged products, and a total of six such metabolites could be identified. We found no hints, however, that this reaction could also occur with thiol-containing macromolecules and lead to covalent binding, and therefore the potential toxicological impact of this pathway remains unclear.

In conclusion, our diverse approaches to studying nifurtimox metabolism have increased substantially our understanding of the biotransformation of this old drug. Our study provides further support for the observation that nifurtimox is extensively degraded and our experiments revealed that nifurtimox is unstable in urine and feces. We identified two major pathways for the degradation of this drug, as well as some evidence of oxidation. The first involves initial reductive nitrofuran activation with many rearranged downstream products or reduction of the hydrazone; it remains unclear whether these pathways have an enzymatic component. The second involves a reaction with thiol-containing nucleophiles (particularly cysteine, and most probably with no enzymatic component) with rearranged or further metabolized downstream products. Information about nifurtimox, the structures of its metabolites, the mechanisms underpinning their formation, and their relative abundance can be used to facilitate the assessment and proposal of possible interactions with other drugs and drug-clearance mechanisms. Notwithstanding the long history of nifurtimox prescribing, undertaking studies to characterize the drug and its metabolites fills gaps in our understanding of its behavior in humans.

■ ASSOCIATED CONTENT

Supporting Information

The Supporting Information is available free of charge at https://pubs.acs.org/doi/10.1021/acs.chemrestox.2c00210.

Methods used for the synthesis and purification of metabolites M-1 to M-5; metabolites identified after incubation of [^{14}C]-nifurtimox with different test systems incorporating different cofactors (NADH, NADPH); and the results of MS/MS fragmentation analysis of metabolite structures, NMR spectra analysis

https://doi.org/10.1021/acs.chemrestox.2c00210
Chem. Res. Toxicol. 2022, 35, 2037−2048

of M-1 to M-5, and chromatographic separations of metabolic reaction products (PDF)

AUTHOR INFORMATION

Corresponding Author

Dieter Lang − *Drug Metabolism and Pharmacokinetics, Bayer AG, 42096 Wuppertal, Germany*; orcid.org/0000-0002-2968-638X; Phone: +49 202 7383 0279; Email: dieter.lang@bayer.com

Authors

Simone I. Schulz − *Bayer AG, 42096 Wuppertal, Germany*

Isabel Piel − *Bayer AG, 42096 Wuppertal, Germany*

Dieudonné T. Tshitenge − *Bayer AG, 42096 Wuppertal, Germany*

Heino Stass − *Bayer AG, 42096 Wuppertal, Germany*

Complete contact information is available at: https://pubs.acs.org/10.1021/acs.chemrestox.2c00210

Author Contributions

CRediT: **Dieter Lang** conceptualization, formal analysis, investigation, methodology, writing-original draft; **Simone I. Schulz** formal analysis, writing-review & editing; **Isabel Piel** formal analysis, writing-review & editing; **Dieudonne T. Tshitenge** formal analysis, writing-review & editing; **Heino Stass** writing-review & editing.

Funding

These studies were supported and funded by Bayer AG.

Notes

The authors declare the following competing financial interest(s): All authors are employees of Bayer AG.

ACKNOWLEDGMENTS

This paper is dedicated to the memory of our colleague Dr. Peter Schmitt. The authors are deeply grateful to him for the analysis and initial interpretation of the NMR spectra. They also thank Melanie Scheinpflug, Andreas Schreiber, and Dirk Gäfke for very skillful, excellent technical work. Highfield Communication, Oxford, U.K. provided medical writing and editorial support in the development of the manuscript, funded by Bayer AG.

ABBREVIATIONS

AcCoA, acetyl-CoA; ADME, absorption, distribution, metabolism, and excretion; AIF, all-ion fragmentation; COSY, COrrelated SpectroscopY; EDTA, ethylenediaminetetraacetic acid; ESI, electrospray ionization; HMBC, heteronuclear multiple bond correlation; HPLC, high-performance liquid chromatography; HRMS, high-resolution mass spectrometry; HSQC, heteronuclear single quantum coherence; iv, intravenous; LSC, liquid scintillation counting; MS, mass spectrometry; NADH, nicotinamide adenine dinucleotide plus hydrogen; NADP, nicotinamide adenine dinucleotide phosphate; NADPH, nicotinamide adenine dinucleotide phosphate plus hydrogen; NMR, nuclear magnetic resonance; ppm, parts per million

REFERENCES

(1) Bern, C. Chagas' Disease. *N. Engl. J. Med.* **2015**, *373*, 456.

(2) Álvarez-Hernández, D.-A.; Franyuti-Kelly, G.-A.; Díaz-López-Silva, R.; González-Chávez, A.-M.; González-Hermosillo-Cornejo, D.; Vázquez-López, R. Chagas disease: current perspectives on a forgotten disease. *Rev. Med. Hosp. Gen. Méx* **2018**, *81*, 154−164.

(3) Bocca Tourres, C. L. Acute period of Chagas' disease and its treatment with Bay 2502. *Bol. Chil. Parasitol.* **1969**, *24*, 24−27.

(4) Wegner, D. H.; Rohwedder, R. W. The effect of nifurtimox in acute Chagas' infection. *Arzneimittelforschung* **1972**, *22*, 1624−1635.

(5) Bayer, A. G. LAMPIT Prescribing Information—August 2020. https://www.accessdata.fda.gov/drugsatfda_docs/label/2020/213464s000lbl.pdf (accessed March 26, 2021).

(6) Altcheh, J.; Castro, L.; Dib, J. C.; Grossmann, U.; Huang, E.; Moscatelli, G.; Pinto Rocha, J. J.; Ramirez, T. E.; on behalf of the CHICO Study Group. Prospective, historically controlled study to evaluate the efficacy and safety of a new paediatric formulation of nifurtimox in children aged 0 to 17 years with Chagas disease one year after treatment (CHICO). *PLoS Neglected Trop. Dis.* **2021**, *15*, No. e0008912.

(7) Pérez Montilla, C. A.; Moroni, S.; González, N.; Moscatelli, G.; Altcheh, J. M.; García Bournissen, F. P38 Identification of Nifurtimox metabolites in urine of pediatric Chagas disease patients by UHPLC-MS/MS. *Arch. Dis. Child.* **2019**, *104*, e32−e33.

(8) Duhm, B.; Maul, W.; Medenwald, H.; Patzschke, K.; Wegner, L. A. Investigations on the pharmacokinetics of nifurtimox- 35 S in the rat and dog. *Arzneimittelforschung* **1972**, *22*, 1617−1624.

(9) Medenwald, H.; Brandau, K.; Schlossmann, K. Quantitative determination of nifurtimox in body fluids of rat, dog and man. *Arzneimittelforschung* **1972**, *22*, 1613−1617.

(10) González-Martin, G.; Paulos, C.; Guevara, A.; Ponce, G. Disposition of nifurtimox and metabolite activity against *Trypanosoma cruzi* using rat isolated perfused liver. *J. Pharm. Pharmacol.* **1994**, *46*, 356−359.

(11) Hall, B. S.; Bot, C.; Wilkinson, S. R. Nifurtimox activation by trypanosomal type I nitroreductases generates cytotoxic nitrile metabolites. *J. Biol. Chem.* **2011**, *286*, 13088−13095.

(12) de Oliveira, I. M.; Bonatto, D.; Pêgas Henriques, J. A. Nitroreductases: Enzymes with Environmental, Biotechnological and Clinical Importance. In *Current Research, Technology and Education Topics in Applied Microbiology and Microbial Biotechnology*; Mendez-Vilas, A., Ed.; Formatex Research Center: Badajoz, 2010; Vol. 2, pp 1008−1019.

(13) Wilkinson, S. R.; Taylor, M. C.; Horn, D.; Kelly, J. M.; Cheeseman, I. A mechanism for cross-resistance to nifurtimox and benznidazole in trypanosomes. *Proc. Natl. Acad. Sci. U.S.A.* **2008**, *105*, 5022−5027.

(14) Stass, H.; Feleder, E.; Garcia-Bournissen, F.; Nagelschmitz, J.; Weimann, B.; Yerino, G.; Altcheh, J. Biopharmaceutical Characteristics of Nifurtimox Tablets for Age- and Body Weight-Adjusted Dosing in Patients With Chagas Disease. *Clin. Pharmacol. Drug Dev.* **2021**, *10*, 542−555.

(15) Letelier, M. E.; Izquierdo, P.; Godoy, L.; Lepe, A. M.; Faundez, M. Liver microsomal biotransformation of nitro-aryl drugs: mechanism for potential oxidative stress induction. *J. Appl. Toxicol.* **2004**, *24*, 519−525.

(16) Nelson, A. C.; Huang, W.; Moody, D. E. Variables in human liver microsome preparation: impact on the kinetics of l-alpha-acetylmethadol (LAAM) n-demethylation and dextromethorphan O-demethylation. *Drug Metab. Dispos.* **2001**, *29*, 319−325.

(17) Stass, H.; Just, S.; Weimann, B.; Ince, I.; Willmann, S.; Feleder, E.; Freitas, C.; Yerino, G.; Munster, U. Clinical investigation of the biopharmaceutical characteristics of nifurtimox tablets − Implications for quality control and application. *Eur. J. Pharm. Sci.* **2021**, *166*, No. 105940.

(18) Castro, G. D.; Lopez, A.; Castro, J. A. Evidence for hydroxyl free radical formation during paraquat but not for nifurtimox liver microsomal biotransformation. A dimethyl-sulfoxide scavenging study. *Arch. Toxicol.* **1988**, *62*, 355−358.

(19) Hanna, P. E.; Anders, M. W. The mercapturic acid pathway. *Crit. Rev. Toxicol.* **2019**, *49*, 819−929.